Proceeding of the 2004 American Control Conference
Boston, Massachusetts June 30 - July 2, 2004

Design and Experimental Evaluation of a Nonlinear Position Controller for a Pneumatic Actuator with Friction

Mark Karpenko and Nariman Sepehri

Abstract— **This paper documents the development and experimental evaluation of a practical nonlinear position controller for a typical industrial pneumatic actuator that gives good performance for both regulating and reference tracking tasks. The system is comprised of a low-cost 5-port proportional valve with flow deadband and a double-rod actuator exhibiting significant friction. Quantitative feedback theory is employed to design a simple fixed-gain PI control law that minimizes the effects of the nonlinear control valve flows, uncertainty in the physical system parameters and variations in the plant operating point. Easy to implement nonlinear modifications to the designed PI control law are then tuned experimentally in a step-by-step fashion to reduce overshoot and to negate the effects of the control valve deadband and actuator friction. Experimental results clearly illustrating the efficacy of the approach are presented.**

I. Introduction

Due to their high force output to weight ratios, cleanliness and comparatively low cost, pneumatic actuators are well suited for a number of industrially relevant tasks ranging from point-to-point positioning to high-accuracy servo positioning and force control. However, complex nonlinear dynamics, compressibility of air, and the parasitic effects of actuator friction continue to make servo control of pneumatic actuators a difficult task.

The nonidealities associated with industrial pneumatic actuators generally complicate the controller design to the extent that it is difficult to achieve reasonable performance using easy to implement proportional-integral (PI) or proportional-integral-derivative (PID) control schemes [1]. A number of authors have, however, proposed nonlinear modifications to conventional control laws that have been shown to dramatically improve the closed-loop performance of pneumatic servos. To name a few, Wang et al. [1] devised a time-delay minimization algorithm aimed at reducing the dead time associated with static friction as well as a null offset compensation scheme for negating the effects of control valve deadband. When used in conjunction with a simple PID control law and acceleration feedback the velocity tracking response of the system was observed to be much improved. Hamiti et al. [2] developed an auto-tuning PI control scheme to eliminate friction induced hunting. Using a high-performance servovalve with negligible deadband, tracking accuracy on the order of 2 mm and steady-state errors around 0.5 mm were reported. Ning and Bone [3] employed a novel proportional plus velocity plus acceleration control law with friction compensation for high-accuracy point-to-point positioning of a pneumatic actuator.

The goal of this work is to develop a practical, yet accurate position controller for an experimental pneumatic actuator. The experimental positioning system is comprised of a low-cost 5-port proportional valve with appreciable deadband and a linear actuator exhibiting significant friction. Whereas previous work seems to focus on either tracking or regulating performance, the primary objective here is to derive a control strategy that gives good fine and coarse positioning performance for both regulating and reference tracking tasks. Towards this objective, quantitative feedback theory (QFT) [4] is first used to design the gains of a PI control law to satisfy pointwise tolerances on the closed-loop frequency response. This enables the selection of the PI control gains that work best with the pneumatic system.

Without modifying the designed PI gains, the relative stability of the designed closed-loop system is improved by replacing the ordinary integrator in the PI control law with a nonlinear reset integrator. Then, to negate the effects of the control valve deadband and actuator friction, which are not considered explicitly in the QFT synthesis, the following nonlinear modifications to the designed resetting PI control strategy are implemented: *(i)* velocity error triggered integral augmentation, and *(ii)* set-point acceleration based overshoot reduction. These modifications, proposed previously by Sepehri et al. [5], were found here to be easy to tune and to afford significant improvements in the closed-loop positioning performance of the experimental pneumatic actuator.

This paper thus makes the following contributions:

1) An accurate and practical nonlinear position controller is developed that overcomes many of the nonidealities in a typical low-cost experimental pneumatic actuator.
2) A systematic approach to the fixed-gain controller design is followed: the well-established QFT design technique is exploited for selection of the best PI controller gains. Nonlinear modifications to the designed PI controller are introduced in a step-by-step fashion to further enhance the closed-loop performance.
3) Experimental results clearly illustrating the efficacy of the approach are presented.

This work was supported by the Natural Sciences and Engineering Research Council of Canada (NSERC).

M. Karpenko and N. Sepehri are with the Department of Mechanical and Industrial Engineering, University of Manitoba, Winnipeg, Manitoba, CANADA R3T 5V6

Correspondence should be sent to N. Sepehri:
nariman@cc.umanitoba.ca

0-7803-8335-4/04/$17.00 ©2004 AACC

II. Experimental Test Rig

The test rig, upon which all experiments were carried out, is shown in Fig. 1. The valve is a low-cost FESTO MPYE-5 series 5-port three-position solenoid driven proportional directional flow control valve and the actuator is a FESTO DNC series double-rod type with a 500 mm stroke. An IBM compatible personal computer equipped with a Metrabyte M5312 quadrature incremental encoder card and a DAS-16F input/output board is used to measure the displacement of the actuator and transmit the software generated control signal to the valve.

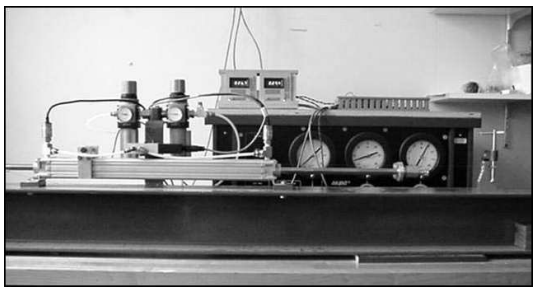

Fig. 1. Experimental test rig.

III. Nonlinear Mathematic Model

A schematic of the experimental test rig for modelling is shown in Fig. 2 along with the variables of interest. Assuming adiabatic charging and discharging of the actuator chambers [6], a set of nonlinear state equations that describe the dynamic system is

$$\begin{aligned}
\dot{x}_p &= v_p \\
\dot{v}_p &= \frac{1}{M}\left(-bv_p + AP_1 - AP_2 - F_f - F_L\right) \\
\dot{P}_1 &= \frac{\gamma RT}{V_1}\dot{m}_1 - \frac{\alpha\gamma P_1 A}{V_1}\dot{x}_p \\
\dot{P}_2 &= -\frac{\gamma RT}{V_2}\dot{m}_2 + \frac{\alpha\gamma P_2 A}{V_2}\dot{x}_p \\
\dot{x}_v &= -\frac{1}{\tau_v}x_v + \frac{k_v}{\tau_v}u
\end{aligned} \tag{1}$$

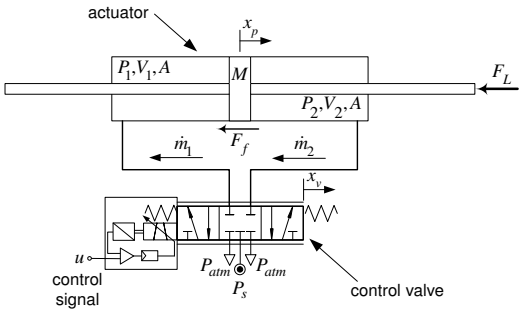

Fig. 2. Schematic of experimental pneumatic actuator.

In (1), x_p is the actuator position and v_p is the actuator velocity. P_1, P_2, V_1, and V_2 are the instantaneous actuator chamber absolute pressures and volumes, respectively. Parameter α is a compressibility flow correction factor, which accounts for the fact that the pressure-volume work process is neither adiabatic nor isothermal but somewhere in between [7]. F_f represents the dry friction force and F_L signifies the externally applied load. The magnitudes of the static friction and Coulomb (sliding friction) were measured experimentally and were found to be approximately 40 N and 20 N, respectively.

As suggested by the manufacturer, the dynamics of the control valve spool are modelled as a first-order lag where the displacement of the valve spool is denoted by x_v and u is the control signal. In the experimental system, the control valve saturates at 5 V input and there exists a flow deadband covering 12% of the range of valve spool displacement.

The nonlinear equation governing the mass flow rate of air through each control valve orifice is [8]

$$\dot{m} = \begin{cases} \frac{C_1 C_d w x_v P_u}{\sqrt{T}} & \text{if } \frac{P_d}{P_u} \le P_{cr} \\ \frac{C_1 C_d w x_v P_u}{\sqrt{T}}\sqrt{1-\left(\frac{P_d/P_u - P_{cr}}{1-P_{cr}}\right)^2} & \text{if } \frac{P_d}{P_u} > P_{cr} \end{cases} \tag{2}$$

where $C_1 = \sqrt{\frac{\gamma}{R}\left(\frac{2}{\gamma+1}\right)^{(\gamma+1)/(\gamma-1)}}$.

In (2), P_d is the absolute downstream pressure, while P_u denotes the absolute upstream pressure. The critical pressure ratio, P_{cr}, which delineates between the sonic (choked) and subsonic flow regimes, was measured experimentally and found to be 0.2.

A suite of experiments was carried out to identify the values of the relevant parameters of the experimental test rig and verify the mathematical model. The remaining model parameters and their identified nominal values are summarized in Table I.

IV. Linear Transfer Function Model

To derive a transfer function representation of the pneumatic actuator dynamics, (2) was linearized using a Taylor series expansion about operating point o. Neglecting the

TABLE I

Identified nominal parameters of experimental test rig.

Parameter	Symbol	Nominal Value
supply pressure	P_s	5 bars
atmospheric pressure	P_{atm}	1 bars
total mass of piston, rods, and load	M	1.91 kg
viscous damping coefficient	b	70 N·sec/m
piston annulus area	A	10.6 cm^2
ideal gas constant	R	287 J/kg·K
temperature of air source	T	300 K
ratio of specific heats	γ	1.4
pressure-volume work correction factor	α	0.89
valve coefficient of discharge	C_d	0.7
valve orifice area gradient	w	22.6 mm^2/mm
valve spool position gain	k_v	0.25 mm/V
valve first-order time constant	τ_v	4.2 msec

second and higher order terms as well as any control valve leakages, the mass flows into each actuator chamber are written as follows

$$\begin{aligned}\Delta\dot{m}_1 &= C_{f1}\Delta x_v - C_{p1}\Delta P_1 \\ \Delta\dot{m}_2 &= C_{f2}\Delta x_v + C_{p2}\Delta P_2\end{aligned} \tag{3}$$

where Δ denotes a perturbation from the operating point value, e.g. $\Delta x_v = x_v - x_{vo}$. Parameters C_{fi} and C_{pi} are known as the valve flow gain and flow-pressure coefficient, respectively. Their specific values depend upon operating point pressures, P_{1o} and P_{2o}, as well as the operating point value of valve spool displacement, x_{vo}. Neglecting control valve deadband and treating the effects of friction as a disturbing load, the transfer function of the open-loop system can be obtained by combining and reducing Laplace transformations of (1) and (3). The transfer function of the open-loop system is

$$X_p(s) = G_1(s)G_2(s)U(s) - G_2(s)\left[F_f(s) + F_L(s)\right] \tag{4}$$

where

$$G_1(s) = \frac{\gamma RTk_vAC_{f1}\left(\gamma RTC_{p2} + V_{2o}s\right)}{\left(\tau_v s+1\right)\left(\gamma RTC_{p1} + V_{1o}s\right)\left(\gamma RTC_{p2} + V_{2o}s\right)} + \frac{\gamma RTk_vAC_{f2}\left(\gamma RTC_{p1} + V_{1o}s\right)}{\left(\tau_v s+1\right)\left(\gamma RTC_{p1} + V_{1o}s\right)\left(\gamma RTC_{p2} + V_{2o}s\right)} \tag{5}$$

and

$$G_2(s) = \frac{\left(\gamma RTC_{p1} + V_{1o}s\right)\left(\gamma RTC_{p2} + V_{2o}s\right)}{D(s)} \tag{6}$$

with

$$\begin{aligned}D(s) = {} & s\left(Ms+b\right)\left(\gamma RTC_{p1} + V_{1o}s\right)\left(\gamma RTC_{p2} + V_{2o}s\right) + \\ & \alpha\gamma A^2 s\left[\gamma RT\left(P_{1o}C_{p2} + P_{2o}C_{p1}\right) + \left(P_{1o}V_{2o} + P_{2o}V_{1o}\right)s\right]\end{aligned} \tag{7}$$

The nonlinear control valve flows, changes in the system operating point, as well as uncertainties in the measurement of any of the physical system parameters give rise to families of representative plant transfer functions, $\mathbf{G}(s) = \mathbf{G_1}(s)\mathbf{G_2}$ and $\mathbf{G_2}(s)$. The ranges and nominal values of the operating point dependant and uncertain model parameters are summarized in Table II.

V. QFT Synthesis of PI Controller

Fig. 3 shows a block diagram of the closed-loop feedback control system. $G_c(s)$ denotes the compensator, which is restricted in this work to have a PI structure. $G_1(s)$ and $G_2(s)$ refer to the uncertain plant transfer functions (5) and (6). Defining loop transmission $L(s) = G_c(s)G_1(s)G_2(s)$, the response of the closed-loop system is written as

$$X_p(s) = \frac{L(s)}{1+L(s)}X_d(s) - \frac{G_2(s)}{1+L(s)}F_d(s) \tag{8}$$

where disturbing force $F_d(s) = \mathscr{L}\left\{F_f(t) + F_L(t)\right\}$. Clearly, $X_p(s)$ varies due to $G_1(s)$ and $G_2(s)$ uncertainty.

The objective of QFT is to synthesize control law $G_c(s)$ to place all the closed-loop frequency responses, $\frac{L(s)}{1+L(s)}$, between lower and upper tracking bounds, $T_L(s)$ and $T_U(s)$,

TABLE II

Ranges and nominal values of operating point dependent and uncertain model parameters.

Uncertain Parameter	Value		
	min	nominal	max
M (kg)	1.81	1.91	2.01
b (N·sec/m)	60	70	80
V_{1o} (m^3) $\times 10^{-4}$	1.32	2.64	3.96
V_{2o} (m^3) $\times 10^{-4}$	1.32	2.64	3.96
τ_v (msec)	3.4	4.2	5.0
P_{1o} (bars)	3.7	3.7	4.5
P_{2o} (bars)	2.3	3.7	3.7
x_{vo} (mm)	0	0	0.125
C_{f1} (kg/sec·m)	8.0	13.6	13.6
C_{f2} (kg/sec·m)	8.0	13.6	13.6
C_{p1} (kg/Pa·sec) $\times 10^{-10}$	0	0	118.6
C_{p2} (kg/Pa·sec) $\times 10^{-10}$	0	0	51.8

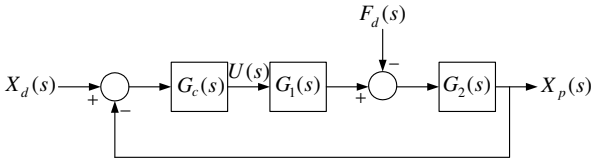

Fig. 3. Single degree-of-freedom feedback structure.

by reducing the control loop sensitivity to plant parametric uncertainty. A suitable frequency domain constraint on the allowable loop transmissions, $\mathbf{L}(s) = G_c(s)\mathbf{G}(s)$, is written in logarithmic form

$$\Delta \log\left|\frac{\mathbf{L}(s)}{1+\mathbf{L}(s)}\right| \le \log\left|\frac{T_U(s)}{T_L(s)}\right| \tag{9}$$

where Δ signifies the variation in the closed-loop transfer function over the entire plant set, $\mathbf{G}(s)$. Closed-loop tracking bounds $T_L(s)$ and $T_U(s)$ were derived from the relevant figures of merit for the step response of a second-order system [9]:

$$\begin{aligned}T_L(s) &= \frac{22500}{(s+5.7)(s+10)^2(s+39.3)} \\ T_U(s) &= \frac{11.81(s+2)(s+20)}{(s+2.1)(s+15)^2}\end{aligned} \tag{10}$$

The time response of $T_L(s)$ is well-damped and has a 90% rise time of 0.7 sec and 2% settling time of 1.0 sec. $T_U(s)$ was selected to have a quicker transient response with a 90% rise time of 0.2 sec, 2% settling time of 0.5 sec and 2 percent overshoot.

To ensure robust stability of the closed-loop system, the following constraint on the peak magnitude of the closed-loop frequency responses is imposed:

$$\left|\frac{\mathbf{L}(s)}{1+\mathbf{L}(s)}\right| \le 1.24 \tag{11}$$

The closed-loop stability specification (11) gives minimum gain and phase margins of 5.14 dB and 45°, respectively. Hence, the peak overshoot in the unit step responses

should not exceed 21%. In a two degree-of-freedom QFT design, prefilter $F(s)$ is available to further shape $\left|\frac{\mathbf{L}(s)}{1+\mathbf{L}(s)}\right|$ to ensure the closed-loop position responses fall within the specified tracking envelope despite the specification of slightly relaxed gain and phase margins. However, in this work, replacing the ordinary integrator with a Clegg-type resetting integrator [10] achieves this result and eliminates the need to design prefilter $F(s)$. Steady-state errors due to disturbances, $F_d(s)$, are zeroed by the integral action of the PI controller.

To proceed with the controller design using QFT, it was first necessary to select a nominal plant $G_{nom}(s)$ from the set $\mathbf{G}(s)$ and then compute QFT bounds, $B(\omega)$, on the nominal loop transmission, $L_{nom}(s) = G_c(s)G_{nom}(s)$. The set of all bounds delineate regions of the Nichols chart where $L_{nom}(s)$ should lie in order to ensure that the closed-loop system performs within the specified tolerances. Fig. 4 shows the relevant bounds and the designed nominal loop transmission $L_{nom}(s)$.

Referring to Fig. 4, $L_{nom}(s)$ was shaped by cascading compensator $G_c(s) = K_p + K_i/s$ in series with $G_{nom}(s)$ and adjusting gains K_p and K_i so that: *(i)* $L_{nom}(s)$ lies on or above the tracking bounds that are single valued functions of the phase angle, and *(ii)* $L_{nom}(s)$ lies exterior to stability bounds that encircle the critical $(-180°, 0$ dB$)$ point. Suitable controller gains were found to be, $K_p = 10$ V/m and $K_i = 26$ V/m·sec.

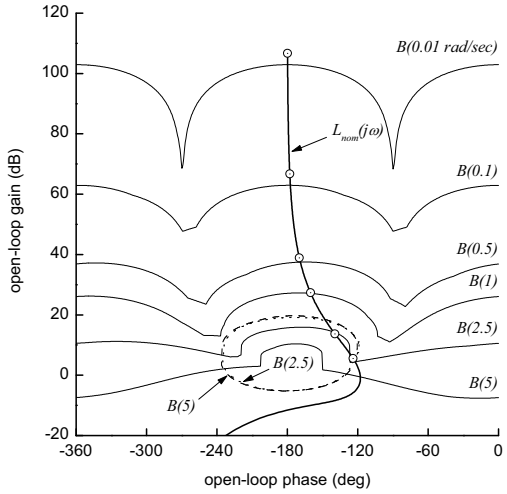

Fig. 4. QFT bounds, $B(\omega)$, and nominal loop transmission, $L_{nom}(j\omega)$ on the Nichols chart.

To verify the design, the closed-loop gain variation, $\Delta \log \left|\frac{\mathbf{L}(s)}{1+\mathbf{L}(s)}\right|$, was calculated at various frequencies. The actual closed-loop gain variation was found to be less than the required tolerance at all frequencies. Thus, the pointwise closed-loop tracking specification (9) is satisfied. However, with reference to Fig. 4, the closed stability bounds are slightly violated. This was a necessary design tradeoff required to properly attenuate resonance in the closed-loop step responses caused by an under-damped complex pole pair present in all $\mathbf{G_2}(s)$.

To further validate the QFT design, the unit step responses corresponding to the linear and Clegg-type resetting designs were simulated. The PI gains obtained from the linear QFT design were used in both control laws. The Clegg integrator [10] is a control element that resets the integral signal to zero whenever the input changes sign. Due to this resetting action, the phase lag of the Clegg integrator is approximately 52° less than that of an ordinary linear integrator [10]. Hence, the potential of the resetting integrator to improve system performance from the point of view of loop stability is apparent.

Referring to Fig. 5a, it is observed that the unit step responses using the linear controller are all stable and that the maximum overshoot is approximately 29%. This is larger than the specified maximum peak overshoot of 21% and is due to penetration of the stability bounds by $L_{nom}(s)$. The tracking bounds are clearly not satisfied by the linear design. In contrast, the peak overshoot in the unit step responses using the resetting control law, Fig. 5b, is less than 8%. This is a significant improvement over the linear design and justifies the use of the resetting control action. The position responses are still seen to fall just outside the tracking bounds. However, as will be seen in Section VI, the experimental step responses fall well within the required envelope so no further design iteration was conducted.

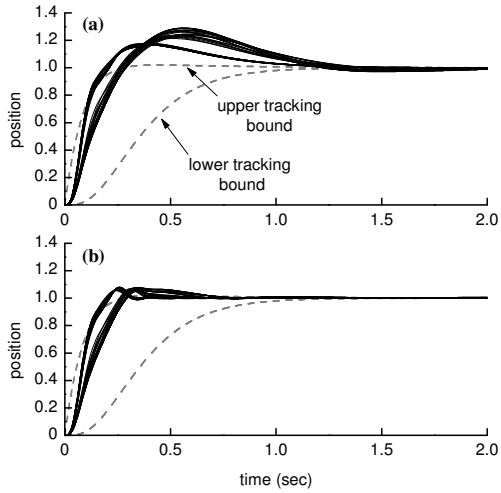

Fig. 5. Simulated closed-loop unit step responses: (a) linear PI control law; (b) resetting PI control law.

VI. Experimentation

Typical experimental step responses with the resetting PI controller are shown in Fig. 6. To prevent friction induced hunting, the rule for resetting the integrator was modified slightly so that the integral was continuously reset whenever the position error, e, fell below a certain threshold, $\varepsilon = 1$ mm. The control strategy was implemented as follows:

$$u(t) = K_p e(t) + K_i I(t) \tag{12}$$

where

$$I(t) = \begin{cases} I(t-\Delta t) + e(t)\Delta t & \text{if } |e(t)| > \varepsilon \\ 0 & \text{if } |e(t)| \le \varepsilon \end{cases} \quad (13)$$

In (12) and (13), u is the control signal, I is the integral signal and parameters $K_p = 10$ V/m and $K_i = 26$ V/m·sec are the same proportional and integral gains obtained from the preceding QFT design.

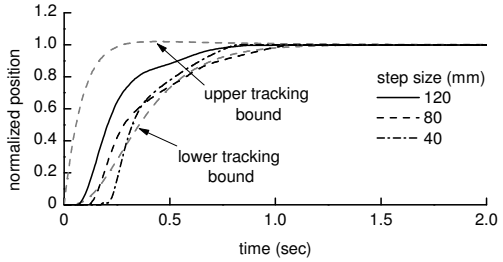

Fig. 6. Typical experimental step responses with resetting control law (12).

Referring to Fig. 6, it is observed that the responses fall within the specified lower and upper tracking bounds. The slight discrepancy between the responses of Fig. 5b and those of Fig. 6 is due to the combined effects of the control valve deadband and actuator static friction. Reasonable speed of response (90% rise times of 0.68 sec) and steady-state positioning errors less than 1 mm were consistently obtained in experiments using the proposed resetting PI control strategy.

The performance of the control system for a typical reference tracking task was examined next. The test signal consisted of a number of *S*-curve trajectories covering 60% of the actuator stroke. Peak actuator velocities were purposefully kept small in an effort to observe the tracking limitations imposed by friction and control valve deadband.

The benchmark performance of the positioning system with resetting PI controller is illustrated in Fig. 7. The integral was reset according to (13), where $\varepsilon = 1.0$ mm only when time derivative of the reference position $\dot{x}_d = 0$. Fig. 7a shows the position response. As expected, significant deadtime (on the order of 0.75 seconds) results from the effects of valve deadband and actuator friction. The peak position error is approximately 50 mm and stick-slip motion is apparent in the response to the small low velocity ramp trajectories. Overshoot is also observed when the rate of change of the reference position, $\dot{x}_d$, is brought to zero.

The following modifications to the designed PI control strategy were implemented next to improve the closed-loop tracking performance: *(i)* velocity error triggered integral augmentation, and *(ii)* set-point acceleration based overshoot reduction. Velocity error triggered integral augmentation reduces the response deadtime resulting from valve deadband and actuator friction via nonlinear conditioning of the integral signal. This scheme, applied initially to improve the position response of a Unimate hydraulic robot in [5],

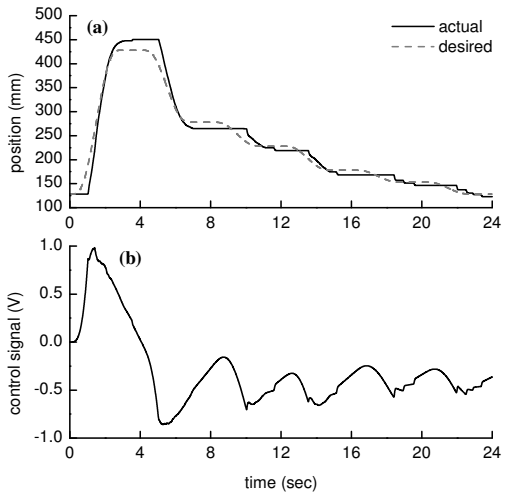

Fig. 7. Benchmark experimental reference tracking performance: (a) position; (b) control signal.

employs a nonlinear filter that estimates the velocity error, $\dot{e}_{db}$, caused by valve deadband and actuator friction. When $\dot{e}_{db}$ exceeds experimental threshold $\dot{e}_{min} = 0.005$ m/sec, the output of the controller is brought to a level necessary to overcome the deadband instead of waiting for the error to accumulate. The nonlinear filter is

$$\dot{e}_{db} = (\dot{x}_p - \dot{x}_d)\frac{\dot{x}_d^2}{\dot{x}_d^2 + \beta \dot{x}_p^2} \quad (14)$$

Constant $\beta = 50$ was found experimentally through trial and error. The resulting position control algorithm was implemented as follows:

$$I(t) = \begin{cases} \frac{-u_{lower} - K_p e(t)}{K_i} & \text{if } \dot{e}_{db} > \dot{e}_{min} \ \&\ u(t) > -u_{lower} \\ I(t-\Delta t) + e(t)\Delta t & \text{if } |\dot{e}_{db}| \le \dot{e}_{min} \\ \frac{u_{upper} - K_p e(t)}{K_i} & \text{if } \dot{e}_{db} > \dot{e}_{min} \ \&\ u(t) < u_{upper} \\ 0 & \text{if } \dot{x}_d(t) = 0 \ \&\ |e(t)| \le \varepsilon \end{cases} \quad (15)$$

In (15), thresholds $u_{lower} = u_{upper} = 0.65$ V were selected experimentally.

The performance of the positioning system with velocity error triggered integral augmentation is illustrated in Fig. 8. As is seen, implementing velocity error triggered integral augmentation significantly reduces the response deadtime. However, overshoot observed during reference tracking tasks remains. To alleviate this, a braking acceleration term was added in the computation of the integral signal. For $|\dot{e}_{db}| \le \dot{e}_{min}$, the integral is now computed as follows:

$$I(t-\Delta t) + e(t)\Delta t + K_a \ddot{x}_{braking}\Delta t \quad (16)$$

where parameter $K_a = 0.15$ sec^2 is a fixed gain tuned by trial and error. The braking acceleration, $\ddot{x}_{braking}$, is calculated from

$$\ddot{x}_{braking} = \begin{cases} \ddot{x}_d & \text{if } \ddot{x}_d \dot{x}_d < 0 \\ 0 & \text{if } \ddot{x}_d \dot{x}_d \ge 0 \end{cases} \quad (17)$$

Equation (17) limits the integrated accelerations to braking accelerations. This reduces the strength of the integral signal when the desired velocity is approaching zero, which is when the problems with overshoot are observed [5].

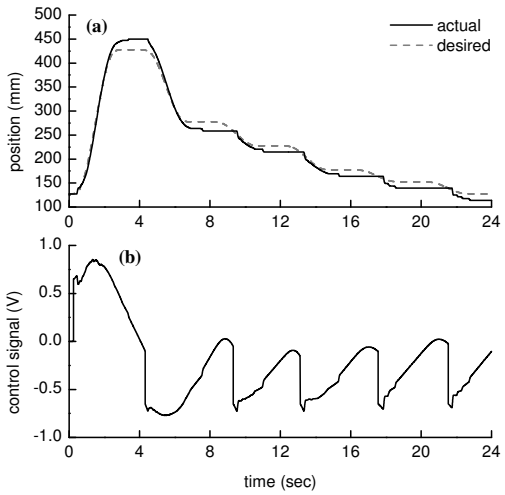

Fig. 8. Experimental reference tracking performance with velocity error triggered integral augmentation: (a) position; (b) control signal.

Fig. 9 shows the experimental responses of the positioning system using the proposed modified Clegg integrator with velocity error triggered integral augmentation and set-point acceleration based overshoot reduction. Parameter ε had to be increased from slightly 1.0 to 4.0 mm to prevent hunting when the actuator was stopped after the *S*-curve input. Referring to Fig. 9, inclusion of the braking acceleration term in the calculation of the integral signal has removed the overshoot and has greatly improved the reference tracking ability of the servopneumatic actuator.

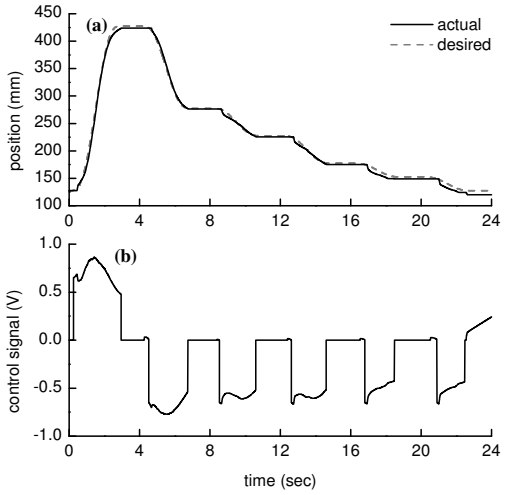

Fig. 9. Experimental reference tracking performance of designed nonlinear PI controller: (a) position; (b) control signal.

VII. Conclusions

A practical, accurate and easy to implement nonlinear position controller for a typical industrial pneumatic actuator with control valve deadband and significant actuator friction has been developed and evaluated experimentally. Design of a fixed-gain PI control law via quantitative feedback theory minimized the effects of the nonlinear control valve flows, changes in the system operating point and uncertainties in the measured plant parameters.

Use of a Clegg-type reset integrator in the designed PI control law was found to improve the relative stability of the closed-loop system. Velocity error triggered integral augmentation and set-point acceleration based overshoot reduction algorithms were implemented in a step-by-step fashion to further enhance the reference tracking performance of the experimental pneumatic actuator despite the parasitic effects of control valve deadband and actuator friction. The experimental results clearly illustrate the efficacy of the proposed fixed-gain nonlinear controller, indicating that experimental regulating errors less than 1 mm could be achieved consistently. Maximum steady errors were observed to increase only slightly to 4 mm for more demanding reference tracking tasks covering 60 percent of the actuator stroke.

References

[1] J. Wang, J. Pu, and P. Moore, "A Practical Control Strategy for Servo-Pneumatic Actuator Systems," *Control Engineering Practice*, vol. 7, pp. 1483-1488, 1999.

[2] K. Hamiti, A. Voda-Besancon, and Roux-Buisson, "Position Control of a Pneumatic Actuator Under the Influence of Stiction," *Control Engineering Practice*, vol. 4, no. 8, pp. 1079-1088, 1996.

[3] S. Ning and G.M. Bone, "High Steady-State Accuracy Pneumatic Positioning System with PVA/PV Control and Friction Compensation," *IEEE International Conference on Robotics and Automation*, Washington, DC, vol. 3, pp. 2824-2829, 2002.

[4] I.M. Horowitz, *Quantitative Feedback Design Theory - QFT*, vol. 1, Boulder, CO: QFT Publications, 1993.

[5] N. Sepehri, A.A. Khayyat, and B. Heinrichs, "Development of a Nonlinear PI Controller for Accurate Positioning of an Industrial Hydraulic Manipulator," *Mechatronics*, vol. 7, no. 8, pp. 683-700, 1997.

[6] S. Liu and J.E. Bobrow, "An Analysis of a Pneumatic Servo System and its Application to a Computer-Controlled Robot," *ASME Journal of Dynamic Systems, Measurement and Control*, vol. 110, no. 3, pp. 228-235, 1988.

[7] E. Richer and Y. Hurmuzlu, "A High Performance Pneumatic Force Actuator System: Part I - Nonlinear Mathematical Model," *ASME Journal of Dynamic Systems, Measurement and Control*, vol. 122, no. 3, pp. 416-425, 2000.

[8] F.E. Sanville, "A New Method of Specifying the Flow Capacity of Pneumatic Fluid Power Valves," *BHRA 2nd International Fluid Power Symposium*, Guildford, England, pp. D3-37-D3-47, 1971.

[9] C.H. Houpis and S.J. Rasmussen, *Quantitative Feedback Theory Fundamentals and Applications*, New York: Marcel Dekker, 1999.

[10] J.C. Clegg, "A Nonlinear Integrator for Servo-Mechanisms," *Transactions of the American Institute of Electircal Engineers Part II - Applications and Industry*, vol. 77, pp. 41-42, 1958.